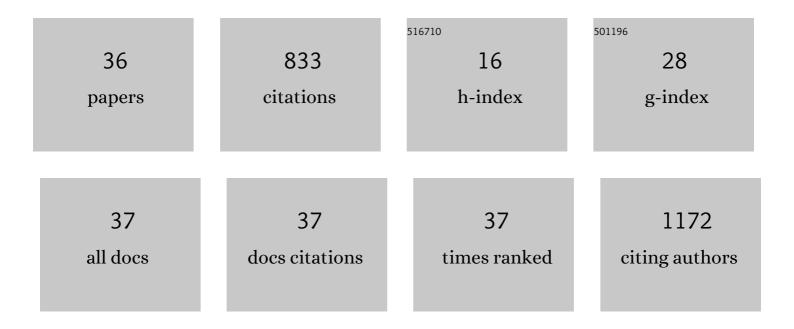
Peter B Kreider

List of Publications by Year in descending order

Source: https://exaly.com/author-pdf/789008/publications.pdf Version: 2024-02-01



#	Article	IF	CITATIONS
1	A graphene film interlayer for enhanced electrical conductivity in a carbon-fibre/PEEK composite. Functional Composite Materials, 2021, 2, .	1.4	16
2	Methane Coupling to Ethylene and Longer-Chain Hydrocarbons by Low-Energy Electrical Discharge in Microstructured Reactors. Industrial & amp; Engineering Chemistry Research, 2021, 60, 6950-6958.	3.7	6
3	The effect of a superhydrophobic coating on moisture absorption and tensile strength of 3D-printed carbon-fibre/polyamide. Composites Part A: Applied Science and Manufacturing, 2021, 145, 106380.	7.6	13
4	Ca/Al doped lanthanum manganite perovskite coated porous SiC for CO2 conversion. Materials Chemistry and Physics, 2020, 253, 123306.	4.0	5
5	Thermochemical CO ₂ splitting performance of perovskite coated porous ceramics. RSC Advances, 2020, 10, 23049-23057.	3.6	11
6	Thermal Model of a Solar Thermochemical Reactor for Metal Oxide Reduction. Journal of Solar Energy Engineering, Transactions of the ASME, 2020, 142, .	1.8	22
7	Effective thermal conductivity of a bed packed with granular iron–manganese oxide for thermochemical energy storage. Chemical Engineering Science, 2019, 207, 490-494.	3.8	14
8	Lattice Expansion in Optimally Doped Manganese Oxide: An Effective Structural Parameter for Enhanced Thermochemical Water Splitting. ACS Catalysis, 2019, 9, 9880-9890.	11.2	29
9	Particle design and oxidation kinetics of iron-manganese oxide redox materials for thermochemical energy storage. Solar Energy, 2019, 183, 17-29.	6.1	28
10	Electrospun Manganese-Based Perovskites as Efficient Oxygen Exchange Redox Materials for Improved Solar Thermochemical CO ₂ Splitting. ACS Applied Energy Materials, 2019, 2, 2494-2505.	5.1	43
11	Reduction kinetics for large spherical 2:1 iron–manganese oxide redox materials for thermochemical energy storage. Chemical Engineering Science, 2019, 201, 74-81.	3.8	22
12	Thermodynamic Analyses of Fuel Production Via Solar-Driven Ceria-Based Nonstoichiometric Redox Cycling: A Case Study of the Isothermal Membrane Reactor System. Journal of Solar Energy Engineering, Transactions of the ASME, 2019, 141, .	1.8	16
13	Analytical Techniques for Probing Small-Scale Layers that Preserve Information on Gas–Solid Interactions. Reviews in Mineralogy and Geochemistry, 2018, 84, 103-175.	4.8	13
14	High-Temperature Gas–Solid Reactions in Industrial Processes. Reviews in Mineralogy and Geochemistry, 2018, 84, 499-514.	4.8	11
15	Gas–Solid Reactions: Theory, Experiments and Case Studies Relevant to Earth and Planetary Processes. Reviews in Mineralogy and Geochemistry, 2018, 84, 1-56.	4.8	39
16	Characterization of Cotton Ball-like Au/ZnO Photocatalyst Synthesized in a Micro-Reactor. Micromachines, 2018, 9, 322.	2.9	6
17	Thermodynamic Analyses of Fuel Production via Solar-Driven Non-stoichiometric Metal Oxide Redox Cycling. Part 1. Revisiting Flow and Equilibrium Assumptions. Energy & Fuels, 2018, 32, 10838-10847.	5.1	28
18	Thermodynamic Analyses of Fuel Production via Solar-Driven Non-stoichiometric Metal Oxide Redox Cycling. Part 2. Impact of Solid–Gas Flow Configurations and Active Material Composition on System-Level Efficiency. Energy & Fuels, 2018, 32, 10848-10863.	5.1	35

Peter B Kreider

#	Article	IF	CITATIONS
19	Nucleation and growth of oriented metal-organic framework thin films on thermal SiO2 surface. Thin Solid Films, 2018, 659, 24-35.	1.8	9
20	Earth-abundant transition metal oxides with extraordinary reversible oxygen exchange capacity for efficient thermochemical synthesis of solar fuels. Nano Energy, 2018, 50, 347-358.	16.0	40
21	Effect of non-stoichiometry on optical, radiative, and thermal characteristics of ceria undergoing reduction. Optics Express, 2018, 26, A360.	3.4	12
22	THERMAL MODELLING OF A SOLAR THERMOCHEMICAL REACTOR FOR METAL OXIDE REDUCTION. , 2018, , .		1
23	Modelling of solar thermochemical reaction systems. Solar Energy, 2017, 156, 149-168.	6.1	52
24	Thermodynamic analysis of a combined-cycle solar thermal power plant with manganese oxide-based thermochemical energy storage. E3S Web of Conferences, 2017, 22, 00102.	0.5	11
25	Plasmonics-enhanced metal–organic framework nanoporous films for highly sensitive near-infrared absorption. Journal of Materials Chemistry C, 2015, 3, 2763-2767.	5.5	41
26	Experimental modeling of hydrogen producing steps in a novel sulfur–sulfur thermochemical water splitting cycle. International Journal of Hydrogen Energy, 2015, 40, 2484-2492.	7.1	6
27	Two-step continuous-flow synthesis of CuInSe ₂ nanoparticles in a solar microreactor. RSC Advances, 2014, 4, 13827-13830.	3.6	7
28	Continuous synthesis of colloidal chalcopyrite copper indium diselenide nanocrystal inks. RSC Advances, 2014, 4, 16418-16424.	3.6	14
29	Surface Modification of Graphite Particles Coated by Atomic Layer Deposition and Advances in Ceramic Composites. International Journal of Applied Ceramic Technology, 2013, 10, 257-265.	2.1	16
30	High-rate synthesis of Cu–BTC metal–organic frameworks. Chemical Communications, 2013, 49, 11518.	4.1	127
31	Visible-light-sensitive Na-doped p-type flower-like ZnO photocatalysts synthesized via a continuous flow microreactor. RSC Advances, 2013, 3, 12702.	3.6	47
32	Visible-light-sensitive nanoscale Au–ZnO photocatalysts. Journal of Nanoparticle Research, 2013, 15, 1.	1.9	35
33	A novel brush feeder for the pneumatic delivery of dispersed small particles at steady feed rates. Powder Technology, 2012, 229, 45-50.	4.2	12
34	Manganese oxide based thermochemical hydrogen production cycle. International Journal of Hydrogen Energy, 2011, 36, 7028-7037.	7.1	32
35	An investigation of a fluidized bed solids feeder for an aerosol flow reactor. Powder Technology, 2010, 199, 70-76.	4.2	10
36	CO ₂ Reduction by Multiple Low-Energy Electric Discharges in a Microstructured Reactor: Experiments and Modeling. Industrial & Engineering Chemistry Research, 0, , .	3.7	4